

Light matter in the core of the Earth: its identity, quantity and temperature using tricritical phenomena

A Aitta

Institute of Theoretical Geophysics, Department of Applied Mathematics and Theoretical Physics, University of Cambridge, Wilberforce Road, Cambridge CB3 0WA, UK

E-mail: A.Aitta@damtp.cam.ac.uk

Abstract. Light elements in the iron-rich core of the Earth are important indicators for the evolution of our planet. Their amount and distribution, and the temperature in the core, are essential for understanding how the core and the mantle interact and for modelling the geodynamo which generates the planetary magnetic field. However, there is a longstanding controversy surrounding the identity and quantity of the light elements. Here, the theory of tricritical phenomena is employed as a precise theoretical framework to study solidification at the high pressures and temperatures where both experimental and numerical methods are complicated to implement and have large uncertainties in their results. Combining the theory with the most reliable iron melting data and the Preliminary Reference Earth Model (PREM) seismic data, one obtains the solidification temperature at the inner core boundary (ICB) for both pure iron and for the alloy of iron and light elements in the actual core melt. One also finds a value of about 2.5 mole% for the amount of light matter. In addition, the density of both solid and liquid pure iron at its melting temperature is found. This allows one to obtain the density of the light matter and thus to identify it to be MgSiO_3 .

Keywords: Phase transitions and critical phenomena, classical phase transitions (theory), phase diagrams (theory), hydrodynamic instabilities

1. Introduction

Although the Earth's core is impossible to reach directly, seismic wave scattering can provide information on the material properties in the deep layers of the Earth. By comparing these to the experimental high pressure studies of various materials, Birch in 1952 was the first to be able to conclude the composition of the Earth's core: "The inner core is most simply interpreted as crystalline iron, the outer part as liquid iron, perhaps alloyed with a small fraction of lighter elements." [1] Several light elements such as H, C, N, O, Mg, Si, P, S, K and some compounds of these have since been considered being present in the core, but the identity and quantity of the light matter has remained unresolved [1-8]. The seismic PREM data [9], known to an accuracy of about 1 %, demonstrates that the density difference between solid and melt at the Earth's ICB is greater than that expected from contraction of matter in solidification, indicating that the core melt has some light elements alloyed with iron, but the densities under high pressure for iron and light elements are much less well established. Direct experimental study of material densities at high pressures and temperatures is difficult and the estimates are based on either shock compression data, whose temperatures are not well-known, or extrapolations using thermal expansion measurements at much lower temperatures (see short summaries in [10, 11]). Theoretical simulations give approximate densities at these extreme pressures, but the results seem to be changing with improving techniques [12, 13]. The uncertainty of these results is increased by the unknown crystal structure which needs to be predetermined for these calculations, and the uncertainty of the iron melting temperature, which, as found by the same technique, in one case [14] is quoted to be about ± 600 K. Reliable and accurate estimates of the

densities of iron and light elements at core pressures and temperatures are essential for success in identifying the core's light matter.

Here a complementary, precise theoretical approach is employed. The theory of tricritical phenomena, extending previous work [15] by further considerations, is used to give an improved estimate of the melting temperature of pure iron over the whole range of core pressures. From this the temperature of iron-rich melt as occurs at the ICB is found. One can then calculate the mole fraction of light matter in the melt, with no input from the iron density. Next, again using the theory of tricritical phenomena, the densities of pure iron, for both solid and melt at the melting temperature, with their uncertainties, are found, at core pressures from the constraint given by PREM on density at the ICB. Finally, one finds the density and the identity of the light matter.

2. The theory of tricritical phenomena for solidification

The density of matter under pressure increases until the distance between atoms becomes less than the atomic diameter; then atoms lose their individuality and the matter changes phase from liquid or solid to plasma where nuclei and electrons are free [16]. This transition from condensed matter to warm dense plasma has been suggested [15] to have a tricritical point where liquid, plasma and solid phases meet. In [15] the melting temperature of material whose melting curve as a function of pressure has a horizontal tangent, was investigated using Landau's theory of tricritical phenomena [16-17]. The theory of tricritical phenomena is applicable to a great variety of physical phenomena, including phase transitions between liquid and crystals [17], and it is known to be very accurate in problems in three spatial dimensions [18-19]. It is also shown to be quantitatively applicable along the phase transition line in a wide neighbourhood around a tricritical point [20]. In the case of a melting curve, the branching out of the vaporization curve and its end point are likely to have their own neighbourhoods outside the validity regime of the tricritical point and its critical line neighbourhood. However, this leaves a large pressure range from room pressure along the melting curve to beyond the tricritical pressure where the theory should be valid, excluding possibly the limited neighbourhoods at a few points where a different curvature can dominate locally in the presence of some triple points related to the transitions to different crystal structures below the melting curve.

One uses an order parameter x to describe first order phase transitions which change to be second order at a tricritical point. $x = 0$ for the more ordered solid phase which occurs at lower temperature, and in the less ordered phases, the liquid or plasma, $x \neq 0$. The Gibbs free energy density is proportional to the Landau potential, which needs to be a sixth order polynomial in x :

$$\Phi(P, T; x) = \frac{1}{6} x^6 + \frac{1}{4} g(P) x^4 + \frac{1}{2} \varepsilon(T) x^2 + \Phi_0(P, T). \quad (1)$$

No higher order terms in x appear in Φ since they can be eliminated using coordinate transformations as in bifurcation theory [21]. This method also scales out any dependence on physical parameters of the coefficient of the highest order term. When the melting curve has a horizontal tangent at high pressures, the coefficients g and ε can be taken to depend linearly on pressure P and temperature T , respectively, and both are equal to 0 at the tricritical point (P_{tc}, T_{tc}) . They are normalized to be

$$g(P) = \frac{P - P_{tc}}{P_{tc}} \quad \text{and} \quad \varepsilon(T) = \frac{3}{16} \frac{T_{tc} - T}{T_{tc} - T_0}, \quad (2)$$

where T_0 is the melting temperature at $P = 0$. The thermodynamically stable state occurs at the value(s) of x that globally minimizes Φ . For different (P, T) values, $\Phi(x)$ can have one, two or three local minima. The temperature T_m of the solid-liquid melting transition is determined by the condition that there are three minima of Φ , all equally deep. This occurs when

$$\varepsilon = 3g^2/16 \quad \text{and} \quad g < 0, \quad (3)$$

giving

$$T_m = T_{tc} - (T_{tc} - T_0)(P_{tc} - P)^2 / P_{tc}^2, \quad \text{for } P < P_{tc}. \quad (4)$$

Below T_m , the solid phase with $x = 0$ is the stable state, but the liquid phase (which corresponds to a local minimum with $x \neq 0$) can exist as an unstable state down to the temperature

$$T_U = T_{tc} - \frac{4}{3}(T_{tc} - T_0)(P_{tc} - P)^2 / P_{tc}^2, \quad \text{for } P < P_{tc} \quad (5)$$

which is where Φ changes from having three minima to having only a single minimum at $x = 0$, and there

$$\varepsilon = g^2/4 \quad \text{with } g < 0. \quad (6)$$

Stable liquid at temperatures lower than T_m can be achieved using impurities: for instance in the familiar eutectic binary phase diagram the melting temperature of the mixture at any concentration is lower than the melting temperature for the closer pure end member. Impurities may stabilize the liquid all the way down to T_U . However, no negative temperature for T_U is possible, as liquids will always solidify at or above absolute zero. Thus there is an absolute lower limit for T_U : at $P = 0$, $T_U = 0$. This gives

$$T_{tc} = 4T_0 \quad (7)$$

which simplifies (4) to

$$T_m = T_0 [4 - 3(P_{tc} - P)^2 / P_{tc}^2], \quad \text{for } P < P_{tc}, \quad (8)$$

and (5) to

$$T_U = 4T_0 [1 - (P_{tc} - P)^2 / P_{tc}^2], \quad \text{for } P < P_{tc}. \quad (9)$$

2.1. On the applicability to other materials

This theory may be applied to other materials than iron which also have a horizontal tangent on their melting curve at high pressure. Unfortunately, there are not usually enough high pressure data to indicate clearly the curvature of the melting curve and its tangent at high pressures, but Cu, Mg, U and possibly Al seem to be promising candidates; however, all are in need of some more high pressure data to provide verification. For Al the curvature of its experimental melting curve at the moment depends crucially on a single shock wave data point whose value and uncertainty is a result of an interpretation of a figure in the original report [22] showing much wider range of uncertainty if one includes the choice for two Grüneisen parameter values than what is expressed in [23] or [24]. If the temperature for this data point were interpreted to be about 3750 K corresponding to a Grüneisen parameter value of 2.0 (as employed in [25] and [26], instead of 2.2 as in [23] and [24]), then it would appear that the melting curve has a horizontal tangent. Then equation (8) above, with the static data [23-24], gives a tricritical point at (97 GPa, 3734 K). Both sides of this tricritical point can be accessed experimentally for evidence of different behaviour on each side. An unexpected behaviour, interpreted as solid-liquid mixed phase, has already been reported [26] at pressures above 125 GPa.

2.2. Critical temperatures for pure iron

Since $T_0 = 1811$ K for pure iron, it follows from (7) that $T_{ic} = 7244$ K. The value for P_{ic} can be estimated using the most reliable high-pressure data for T_m (the same data [27-33] as selected earlier [15]). This gives $P_{ic} = (608 \pm 6)$ GPa, about 200 GPa less than the estimate found previously where both T_{ic} and P_{ic} were simultaneously determined without utilizing (7). Figure 1 shows the best fit (solid line) with its uncertainty (dashed lines) and the data with their error bars. Also, T_U is shown in figure 1 (the lower solid line), with its uncertainty (dashed lines). From (8) and (9), one finds that at $P = 329$ GPa, the ICB pressure, $T_m = (6100 \pm 30)$ K and $T_U = (5710 \pm 40)$ K, whose uncertainties follow from the uncertainty in P_{ic} . This pure iron melting temperature T_m is between the cluster of estimates around 6000 K obtained by various methods [34] and (6350 ± 600) K found in ab initio calculations [14]. T_U determines the absolute lower limit down to which any impurities in the iron-rich core melt can lower the melting temperature. Its value is very close to 5700 K, the value inferred for the temperature at the ICB from ab initio calculations on the elasticity properties of the inner core [35], and is consistent with the range 5400 K – 5700 K reported in [14]. The temperature difference $T_m - T_U = (383 \pm 9)$ K at ICB is less than, for instance, the estimate 600 K to 700 K in [14] but more than the 300 K used in the rather recent energy budget calculations of the core [36].

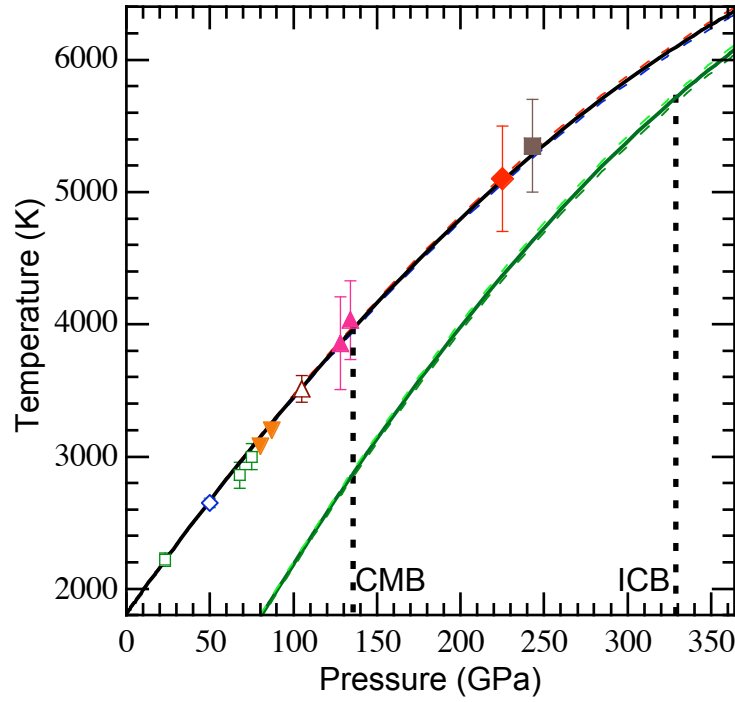


Figure 1. Iron melting temperature T_m as a function of pressure P as calculated from equation (8) (upper solid line) with its maximum uncertainty (dashed lines) and the consistent experimental data whose selection details are discussed in [15]. Open symbols are for the most accurate static measurements (squares [27]; diamond [28]; triangle [29]). Solid symbols show all the supporting shock wave results (downward triangles [30]; triangles [31]; diamond [32], square [33]). Error bars are from the original sources, but [30] gave none. The limit for liquid temperature, T_U , as a function of pressure P as calculated from equation (9) (lower solid line) with its maximum uncertainty (dashed lines). The core boundary pressures are shown by vertical dotted lines.

2.3. Critical concentration at ICB

For a small (less than about 5 atomic %) amount of impurities, an iron-dominated alloy can be approximated by an ideal solution. Then the iron concentration c_{Fe} can be related to the alloy's chemical potential and that of pure iron by $\mu_{\text{alloy}} = \mu_{\text{Fe}} + RT \ln c_{\text{Fe}}$ (see, for instance, [37]). On the other hand, chemical potential is Gibbs free energy per mole and thus proportional to the Landau potential (1): $\mu = \frac{128}{3} L_0 \Phi$, where the proportionality coefficient determined in previous work [15] is simplified by using (7) and the latent heat L_0 at zero pressure. When the liquid temperature equals T_U , $\Phi_{\text{alloy}} = \Phi_0$ (corresponding to having three equally deep minima in the potential) and $\Phi_{\text{Fe}} = \Phi_0 - g(P_{\text{ICB}})^3 / 48$ which follows from (6) and (1) with $x^2 = -g(P_{\text{ICB}})/2$. The

concentration for the impurities is therefore $c_i = 1 - c_{\text{Fe}} = 1 - \exp\left[-\frac{8L_0}{9RT_U} \left(\frac{P_{\text{ic}} - P_{\text{ICB}}}{P_{\text{ic}}}\right)^3\right]$ giving c_i

$= (2.47 \pm 0.07)$ mole%, where the uncertainty corresponds to the maximum uncertainty in P_{ic} and T_U . Thus, by this method, one can find the concentration of light elements at the ICB

without using the iron density, which is not known very accurately. The small fraction of Ni expected also in the core is here assumed not to change the iron behaviour due to the remarkable similarities of these atoms.

2.4. Critical densities at ICB

In order to identify the light matter, the iron melt density needs to be approximated. The theory of the tricritical point gives an equation similar to (4) for the density of the liquid at its melting temperature, $\rho_m = \rho_{tc} - (\rho_{tc} - \rho_0)(P_{tc} - P)^2 / P_{tc}^2$, for $P < P_{tc}$, where ρ_0 is the zero pressure liquid density and ρ_{tc} is the liquid density at P_{tc} , both at their melting temperature. For pure iron, the liquid state exists as an unstable state relative to the solid for densities down to

$\rho_U = \rho_{tc} - \frac{4}{3}(\rho_{tc} - \rho_0)(P_{tc} - P)^2 / P_{tc}^2$, for $P < P_{tc}$. Below ρ_U only solid state is possible. However, light elements dissolved into the iron-rich core melt can generate densities less than that of pure iron. Here ρ_U is identified to be the density of the light-element enriched iron melt at ICB and its value $\rho_U = \rho_m^{\text{PREM}}(P_{\text{ICB}})$ is known from PREM (cf. T_U was identified to be the temperature there). This gives, with P_{tc} found above, $\rho_{tc} = (14.20 \pm 0.14) \text{ g/cm}^3$, where the uncertainty corresponds to the range obtained using $\pm 1\%$ uncertainty in PREM combined with the uncertainty in P_{tc} . This density is consistent within the uncertainties of the similar densities at high pressure for iron's principal Hugoniot in [38], [39] and the older data tabulated in [40] even though the temperatures they correspond to are not known and need not be the melting temperature. According to [41] the very high-pressure measurements (beyond 620 GPa in [42], that is, beyond P_{tc} found here) extend into the regime of increasing thermal ionization. Figure 2 presents ρ_m as a thin solid line and ρ_U as a dot-dashed line, together with the PREM density data as a thicker solid line. In particular, at ICB, $\rho_m = (12.67 \pm 0.07) \text{ g/cm}^3$, about 4.1 % higher than ρ_m^{PREM} and 0.7 % lower than the PREM density of the solid ρ_s^{PREM} .

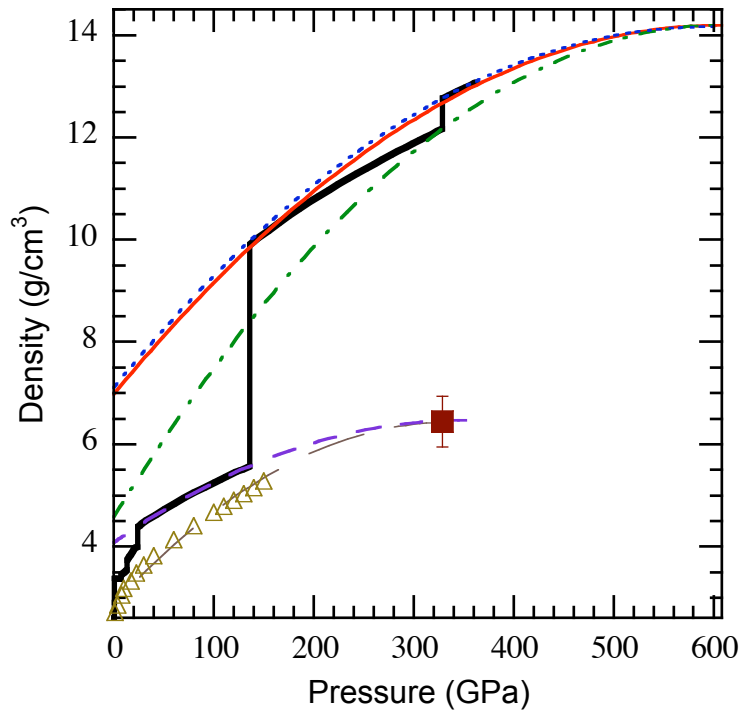


Figure 2. Densities as a function of pressure up to P_{tc} . Density of solid iron ρ_s (dotted line) and liquid iron ρ_m (thin solid line) at their melting temperature with the limit for liquid density ρ_U (dashed-dotted line) and PREM [9] density (thick solid line). Square shows the density found here for the light matter $MgSiO_3$ in the melt at the inner core boundary. To demonstrate its reasonability it is connected by quadratic fits to both PREM lower mantle densities (dashed line) and to the new data [53] (triangles) for liquid $MgSiO_3$ density at its melting temperature (long dashed line).

One also finds that at the CMB, ρ_U is close to 1 % below ρ_m^{PREM} , indicating that the core melt hardly has light impurities there or some Ni compensates them in the melt. This is about 8 % less than obtained from ab initio calculations (see, for instance, [13]) which at that pressure also give about 10 % (or 6 % with free energy correction) greater temperatures for the melting [12, 14]. But the value of ρ_U is in full agreement with the similarity of compressional wave velocity measurements against density in pure Fe and seismic velocity profile against density from PREM at the pressures of the upper outer core [43]. This means that light matter brought to CMB by convection is removed from the melt by solidification accompanied by some iron. From (8) the melting temperature T_m at the CMB pressure is (3965 ± 20) K, very similar to its seismic estimate (3950 ± 200) K [44]. This is further evidence that at the CMB the core melt is solidifying, as has been suggested in [45-47]. Even though there is presently no experimental evidence concerning the solidification temperature of relevant matter from iron-rich melt at the CMB pressure, the temperature must be close to the pure iron melting temperature owing to the very small amount of impurities.

The volume contraction (from [15] with (7) and using L_0) in solidification, $\Delta V = 6L_0(P_{tc} - P)^2 / P_{tc}^3$, is (0.0288 ± 0.0004) cm³/mol for iron at ICB pressure, which is less than an estimate of 0.055 cm³/mol used for ϵ -iron in [48]. One can find the density ρ_s of pure

solid iron from the density of the melt ρ_m using $\rho_s = A/(A/\rho_m - \Delta V)$, where the atomic weight A is taken to be the standard value for iron on the Earth. ρ_s is shown in figure 2 as a dotted line. In particular, at ICB, $\rho_s = (12.758 \pm 0.006) \text{ g/cm}^3$ whose uncertainty only takes account of the uncertainties in ρ_m and ΔV . The upper end of the uncertainty range includes ρ_s^{PREM} indicating that the inner core is very nearly pure iron. These results give a smaller than traditionally expected (10 ± 5) % density deficit relative to pure iron but rather close to the prediction of 5.4 % in [48].

3. Light matter content, density and identification

The average density of the impurities ρ_i at ICB can be estimated using the equation

$$\frac{1}{\rho_m^{\text{PREM}}} = \frac{y}{\rho_i} + \frac{1-y}{\rho_m},$$

where y is the weight fraction of the impurities, valid strictly for

homogeneous solutions but probably also for the fluid in the core due to the very small amount of impurities present and the very long time the core melt has been mixed by convection. In figure 3, y and ρ_i are presented as a function of molar mass for $c_i = 2.47$ mole% as was obtained earlier. No single light element has a high enough ρ_i [40] in agreement with previous research [4, 7, 14] which suggests that the light matter needs to have at least two elements. The previously suggested two likely elements O and Si [14, 49-51] if combined as SiO_2 also generates too low ρ_i [40]. Thus it becomes important to expand the search to the common three-element compounds, particularly the most abundant mantle compounds forsterite, Mg_2SiO_4 , and magnesium silicate, MgSiO_3 . If the compound were forsterite, one obtains $\rho_i = 7.5 \text{ g/cm}^3$ which seems to be too high [52-53], but if it were MgSiO_3 , then $\rho_i = (6.5 \pm 0.5) \text{ g/cm}^3$, and this result is very reasonable [53]. Even though the density of any light element or compound at ICB conditions is not known accurately, using this latter value of ρ_i one can find a smooth second order continuation of the new density estimates in [53] for liquid MgSiO_3 at its melting temperature. This ρ_i can also be quadratically aligned with the PREM lower mantle densities of solid material which is believed to be dominated by MgSiO_3 . ρ_i for MgSiO_3 and these two fits are shown in figure 2. For MgSiO_3 , $y = (4.36 \pm 0.13) \text{ wt}\%$ implying that at ICB the melt has about 1.06 wt% of Mg, 1.22 wt% Si and 2.09 wt% O. The amount of the light matter found by this method is less than the recent results in [14] and [43], however, the iron density used in those calculations is over 2 % higher than that found here. This implies their need to include some light elements in the inner core, too.

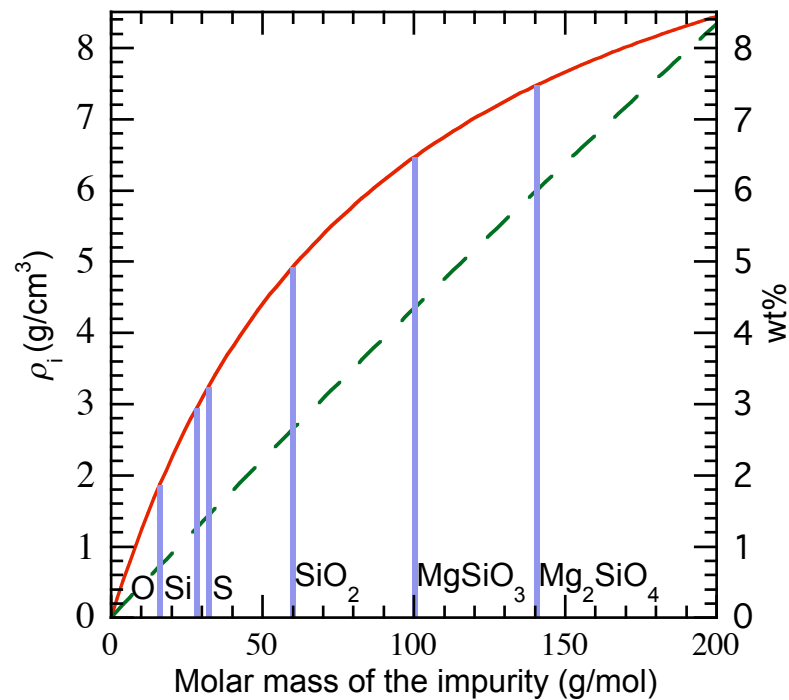


Figure 3. Density and weight fraction of the impurities as a function of molar mass for the obtained impurities' mole fraction 0.0247. To guide the eye, the mole fractions for O, Si, S, SiO₂ and the main mantle components MgSiO₃ and Mg₂SiO₄ are shown by vertical lines.

The light matter found here suggests that in the partially or fully molten early Earth, a small quantity of the molten main mantle material accompanied the iron when it descended as a melt to the core. The compound MgSiO₃ has in the past [49, 54] been considered as the core's light compound, and so have each of its elements. In particular, Si and O, alone or together, have been often suggested as light elements in the core. Magnesium has been suggested more rarely: it was suggested by Alder in 1966 [54] but later discounted on account of the weak solubility of MgO in iron melt even at high pressures [4]. However, recently Mg has been found adequately soluble in iron at high pressures and thus suggested as an important light element in the core [55]. The result found here calls for further investigations of the liquid density of Fe, Ni and MgSiO₃, both pure and as alloys, at core conditions. It will also be worth investigating the crystal structure and the Fe-concentration of the solid, and especially the solidification temperature, as a small amount of molten MgSiO₃ in Fe, or in Fe-Ni, is cooled down at the CMB pressure.

4. Conclusions

The theory of tricritical phenomena provides a concise framework to calculate precisely the quantities essential to understand the Earth's core. Accurate quantitative predictions are obtained for the iron melting temperature and melting density at high pressures, and for the temperature and the amount and identity of the light matter in the real Earth at the inner core

boundary. The density of the solid inner core is found to be similar to pure iron. The density of light matter in the melt corresponds to MgSiO_3 . Thus the core consists of the four most abundant elements of the Earth in addition to the commonly expected Ni not considered here separately. It is likely that the small amount of MgSiO_3 originates from the molten early mantle. This result agrees with the understanding that O is the principal light element in the core, and the expectation that the core has some Si. Additionally this work identifies the third main light element to be Mg. This challenges the present geochemical calculations where no O or Mg is assumed in the core. Furthermore, this study indicates that the light matter solidifies out at CMB with some iron, in agreement with previous suggestions.

Acknowledgement

I thank Paul Asimow for providing me with reference [53] in a tabulated form.

References

1. Birch F, *Elasticity and constitution of the Earth's interior*, 1952 *J. Geophys. Res.* **57** 227
2. Stevenson D J, *Models of the Earth's Core*, 1981 *Science* **214** 611
3. Jeanloz R, *The nature of the Earth's core*, 1990 *Annu. Rev. Earth Planet. Sci.* **18** 357
4. Poirier J-P, *Light elements in the Earth's outer core: A critical review*, 1994 *Phys. Earth Planet. Inter.* **85** 319
5. Li J and Fei Y, *Experimental constraints on core composition*, 2003 *The Mantle and Core*, ed. R. W. Carlson Vol. 2 Treatise on Geochemistry (Oxford: Elsevier-Pergamon) p. 1
6. McDonough W F, *Compositional model for the Earth's core*, 2003 *The Mantle and Core*, ed. R. W. Carlson Vol. 2 Treatise on Geochemistry (Oxford: Elsevier-Pergamon) p. 547
7. Wood B J, Walter M J and Wade J, *Accretion of the Earth and segregation of its core*, 2006 *Nature* **441** 825
8. Georg R B, Halliday A N, Schauble E A and Reynolds B C, *Silicon in the Earth's core*, 2007 *Nature* **447** 1102
9. Dziewonski A M and Anderson D L, *Preliminary reference Earth model*, 1981 *Phys. Earth Planet. Inter.* **25** 297
10. Chen B, Gao L, Funakoshi K-i and Li J, *Thermal expansion of iron-rich alloys and implications for the Earth's core*, 2007 *Proc. Natl. Acad. Sci. USA* **104** 10.1073/pnas.0610474104

11. Dewaele A, Loubeyre P, Occelli F, Mezouar M, Dorogokupets P I and Torrent M, *Quasihydrostatic equation of state of iron above 2 Mbar*, 2006 *Phys. Rev. Lett.* **97** 215504
12. Alfè D, Price G D and Gillan M J, *Iron under Earth's core conditions: Liquid-state thermodynamics and high-pressure melting curve from ab initio calculations*, 2002 *Phys. Rev. B* **65** 165118
13. Koc̃i L, Belonoshko, A B and Ahuja R, *Molecular dynamics study of liquid iron under high pressure and high temperature*, 2006 *Phys. Rev. B* **73** 224113
14. Alfè D, Gillan M J and Price G D, *Temperature and composition of the Earth's core*, 2007 *Contemp. Phys.* **48** 63
15. Aitta A, *Iron melting curve with a tricritical point*, 2006 *J. Stat. Mech.* **2006** P12015
16. Landau L D and Lifshitz E M, 2001 *Statistical Physics Part 1*, 3rd edn (Oxford: Butterworth-Heinemann)
17. ter Haar D (ed), 1965 *Collected Papers of L. D. Landau* (London: Pergamon) p. 193
18. Pfeuty P and Toulouse G, 1977 *Introduction to the Renormalization Group and to Critical Phenomena* (London: Wiley)
19. Lawrie I D and Sarbach S, *Theory of tricritical points*, 1984 *Phase Transitions and Critical Phenomena* vol. 9, ed C Domb and J Lebowitz (London: Academic Press)
20. Aitta A, *Quantitative Landau model for bifurcations near a tricritical point in Couette-Taylor flow*, 1986 *Phys. Rev. A* **34** 2086
21. Golubitsky M and Schaeffer D G, 1985 *Singularities and Groups in Bifurcation Theory* vol I (New York: Springer)
22. Shaner J W, Brown J M and McQueen R G, *Melting of metals above 100 GPa*, 1984 *Mater. Res. Soc. Symp. Proc.* **22** 137
23. Boehler R and Ross M, *Melting curve of aluminum in a diamond cell to 0.8 Mbar: implications for iron*, 1997 *Earth Planet. Sci. Lett.* **153**, 223
24. Hänström A and Lazor P, *High pressure melting and equation of state of aluminium*, 2000 *J. Alloys Compounds* **305** 209
25. McQueen R G, Fritz J N and Morris C E, *The velocity of sound behind strong shock waves in 2024 Al*, 1984 *Shock Waves in Condensed Matter – 1983*, ed. J R Asay, R A Graham and G K Straub (Amsterdam: Elsevier) p. 95

26. Yu Y-Y, Tan H, Hu J-B and Dai C-D, *Shear modulus of shock-compressed LY12 aluminium up to melting point*, 2008 *Chin. Phys. B* **17** 264
27. Shen G, Mao H-k, Hemley R J, Duffy T S and Rivers M L, *Melting and crystal structure of iron at high pressures and temperatures*, 1998 *Geophys. Res. Lett.* **25** 373
28. Shen G, Prakapenka V B, Rivers M L and Sutton S R, *Structure of liquid iron at pressures up to 58 GPa*, 2004 *Phys. Rev. Lett.* **92** 185701
29. Ma Y, Somayazulu M, Shen G, Mao H-k, Shu J and Hemley R J, *In situ X-ray diffraction studies of iron to Earth-core conditions*, 2004 *Phys. Earth Planet. Inter.* **143–144** 455
30. Sun Y-H, Huang H-J, Liu F-S, Yang M-X and Jing F-Q, *A direct comparison between static and dynamic melting temperature determinations below 100 GPa*, 2005 *Chin. Phys. Lett.* **22** 2002
31. Tan H, Dai C D, Zhang L Y and Xu C H, *Method to determine the melting temperatures of metals under megabar shock pressures*, 2005 *Appl. Phys. Lett.* **87** 221905
32. Nguyen J H and Holmes N C, *Melting of iron at the physical conditions of the Earth's core*, 2004 *Nature* **427** 339
33. Brown J M and McQueen R G, *Phase transitions, Grüneisen parameter, and elasticity for shocked iron between 77 GPa and 400 GPa*, 1986 *J. Geophys. Res.* **91** 7485
34. Anderson O L, Isaak D G and Nelson V E, *The high-pressure melting temperature of hexagonal close-packed iron determined from thermal physics*, 2003 *J. Phys. Chem. Solids* **64** 2125
35. Steinle-Neumann G, Stixrude L, Cohen R E and Gülseren O, *Elasticity of iron at the temperature of the Earth's inner core*, 2001 *Nature* **413** 57
36. Lister J R, *Expressions for the dissipation driven by convection in the Earth's core*, 2003 *Phys. Earth Planet. Inter.* **140** 145
37. Porter D A and Easterling K E, 1997 *Phase Transformations in Metals and Alloys*, 2nd edn (London: Chapman & Hall)
38. Brown J M, *The equation of state of iron to 450 GPa: another high pressure solid phase?* 2001 *Geophys. Res. Lett.* **28** 4339
39. Koenig M, Benuzzi-Mounaix A, Ravasio A, Vinci T, Ozaki N, Lepape S, Batani D, Huser G, Hall T, Hicks D, MacKinnon A, Patel P, Park H S, Boehly T, Borghesi M, Kar S and Romagnani L, *Progress in the study of warm dense matter*, 2005 *Plasma Phys. Control. Fusion* **47** B441

40. Kogan V E, Levashov P R and Lomov I N, *Shock wave database*, 2003
<http://www.ihed.ras.ru/rusbank/>.
41. Brown J M, Fritz J N and Hixson R S, *Hugoniot data for iron*, 2000 *J. Appl. Phys.* **88** 5496
42. Al'tshuler L V, Bakanova A A, Dudoladov I P, Dynin E A, Trunin R F and Chekin B S, *Shock adiabatic curves of metals*, 1981 *J. Appl. Mech. Tech. Phys.* **22** 145
43. Badro J, Fiquet G, Guyot F, Gregoryanz E, Occelli F, Antonangeli D and d'Astuto M, *Effect of light elements on the sound velocities in solid iron: Implications for the composition of Earth's core*, 2007 *Earth Planet. Sci. Lett.* **254** 233
44. van der Hilst R D, de Hoop M V, Wang P, Shim S-H, Ma P and Tenorio L, *Seismostratigraphy and thermal structure of Earth's core-mantle boundary region*, 2007 *Science* **315** 1813
45. Schloessin H H and Jacobs J A, *Dynamics of a fluid core with inward growing boundaries*, 1980 *Can. J. Earth Sci.* **17** 72
46. Buffett B A, Garnero E J and Jeanloz R, *Sediments at the top of Earth's core*, 2000 *Science* **290** 1338
47. Buffett B, Garnero E and Jeanloz R, *Porous sediments at the top of Earth's core? Response*, 2001 *Science* **291** 2091
48. Anderson O L and Isaak D G, *Another look at the core density deficit of Earth's outer core*, 2002 *Phys. Earth Planet. Inter.* **131** 19
49. Knittle E and Jeanloz R, *Earth's core-mantle boundary: Results of experiments at high pressures and temperatures*, 1991 *Science* **251**, 1438
50. Takafuji N, Hirose K, Mitome M and Bando Y, *Solubilities of O and Si in liquid iron in equilibrium with (Mg,Fe)SiO₃ perovskite and the light elements in the core*, 2005 *Geophys. Res. Lett.* **32** L06313
51. Sakai T, Kondo T, Ohtani E, Terasaki H, Endo N, Kuba T, Suzuki T and Kikegawa T, *Interaction between iron and post-perovskite at core-mantle boundary and core signature in plume source region*, 2006 *Geophys. Res. Lett.* **33** L15317
52. Mosenfelder J L, Asimow P D and Ahrens T J, *Thermodynamic properties of Mg₂SiO₄ liquid at ultra-high pressures from shock measurements to 200 GPa on forsterite and wadsleyite*, 2007 *J. Geophys. Res.* **112** B06208
53. Mosenfelder J L, Asimow P D, Frost D J, Rubie D C and Ahrens T J, *Constraints on thermodynamics of the lower mantle from new shock-wave experiments in the MgSiO₃*

and Mg_2SiO_4 systems, 2007 *EOS Trans. AGU* **88**(52), Fall Meet. Suppl., Abstr. MR54A-02

54. Alder B J, *Is the mantle soluble in the core?* 1966 *J. Geophys. Res.* **71** 4973
55. Dubrovinskaia N, Dubrovinsky L, Kantor I, Crichton W A, Dmitriev V, Prakapenka V, Shen G, Vitos L, Ahuja R, Johansson B and Abrikosov I A, *Beating the miscibility barrier between iron group elements and magnesium by high-pressure alloying*, 2005 *Phys. Rev. Lett.* **95** 245502